Electronic Supplementary Information (ESI) for

Selective loading of platinum or silver cocatalyst onto a hydrogen-evolution photocatalyst in a silver-mediated all solid-state Z-scheme system for enhanced overall water splitting

Junya Osaki, [a] Masaomi Yoda, [b] Toshihiro Takashima [ab] and Hiroshi Irie *[ab]

[a]*Special Doctoral Program for Green Energy Conversion Science and Technology, Integrated Graduate School of Medicine, Engineering, and Agricultural Sciences, University of Yamanashi, 4-3-11 Takeda, Kofu, Yamanashi 400-8511, Japan.*
[b]*Clean Energy Research Center, University of Yamanashi, 4-3-11 Takeda, Kofu, Yamanashi 400-8511, Japan.*

Contents

ESI-1) Detailed preparation and characterization procedures.

A powdered photocatalyst composed of $ZnRh_2O_4$, $Bi_4V_2O_{11}$, and Ag ($ZnRh_2O_4$/Ag/$Bi_4V_2O_{11}$) was prepared using the following method. First, $ZnRh_2O_4$ and $Bi_4V_2O_{11}$ powders were synthesized using a solid-state reaction method. As starting materials, commercial ZnO (Wako, purity 99.0%) and Rh_2O_3 powders (Kanto Kagaku, purity 99.9%) were used for $ZnRh_2O_4$, and Bi_2O_3 (Kanto Kagaku, purity 99.9%) and V_2O_5 powders (Kanto Kagaku, purity 99.0%) were used for $Bi_4V_2O_{11}$. Stoichiometric amounts of the starting materials for both materials were wet-ball-milled for 20 h in polyethylene bottles using zirconium dioxide (ZrO_2) balls as the milling medium. The resulting mixtures were calcined at 1150 °C for 24 h and 850 °C for 8 h to obtain $ZnRh_2O_4$ and $Bi_4V_2O_{11}$ powders, respectively, which were then thoroughly ground. Only the $Bi_4V_2O_{11}$ powder was subsequently soaked and stirred in distilled water for 20 h, followed by filtration and drying at 65°C for 12 h.

The obtained $ZnRh_2O_4$ and $Bi_4V_2O_{11}$ powders and commercial Ag_2O powder, with a molar ratio of 1.0:1.2:1.0, were wet-ball-milled as described above. The mixed powders were pressed into pellets by applying a force of 60 kN, and the obtained pellets were heated at 750°C for 2 h. After grinding the pellets into a fine powder, the powder was soaked in a 3 M nitric acid (HNO_3, Kanto Kagaku) aqueous solution for 5 min. The powder was then filtered and washed thoroughly with distilled water and dried at 65°C for 12 h.

Photodeposition of Pt was conducted by first dispersing 80 mg $ZnRh_2O_4$/Ag/$Bi_4V_2O_{11}$ in 40 mL formaldehyde solution (25 vol%) containing 10 mL of 8.65 mM hexachloroplatinic acid ($H_2PtCl_6 \cdot 6H_2O$, >98.5%; Kanto Kagaku) solution as the source of Pt. The suspension was then deaerated using liquid nitrogen (N_2) and illuminated by a light-emitting diode (LED) lamp with a wavelength of 850 nm (LEDH60-850; Hamamatsu Photonics) equipped with an optical filter (IR85N; HOYA) for 35 h under constant stirring. This light condition was used for the selective photo-excitation of $ZnRh_2O_4$ due to its band-gap energy of 1.2 eV, which is lower than that of $Bi_4V_2O_{11}$, which has a band-gap of 1.7 eV. The resulting sample was obtained by filtration, washed, and dried at 80 °C overnight. For the photodeposition of Ag, 80 mg $ZnRh_2O_4$/Ag/$Bi_4V_2O_{11}$ was dispersed in 40 mL formaldehyde solution (25 vol%) containing 10 mL of 18 mM silver nitrate ($AgNO_3$, >99%; Kanto Kagaku) solution as the source of Ag. The suspension was then deaerated using liquid N_2 and illuminated using the 850-nm LED equipped with the IR85N optical filter for 20 h under stirring.

The crystal structures of the prepared powders were determined by X-ray diffraction (XRD) using a PW-1700 instrument (PANalytical). UV-visible absorption (UV-vis) spectra were obtained by the diffuse reflection method using a spectrometer (V-650, Jasco) with barium sulfate ($BaSO_4$) as the reflectance standard. The Bi 4f, V 2p, Zn 2p, Rh 3d, Ag 3d, and Pt 4f core levels were measured by X-ray photoelectron spectroscopy (XPS; Axis-Ultra, Shimadzu). The peaks were calibrated using the C 1s peak derived from a hydrocarbon surface contaminant with a binding energy of 284.6 eV. To quantitatively evaluate the valency and percentages of Ag and Pt contained in the photocatalysts, peak deconvolution was performed using a Gaussian lineshape. A scanning electron microscope (SEM, JSM-6500F, JEOL) was used to observe the morphology of the prepared photocatalysts. A scanning transmission electron microscope (STEM, Tecnai Osiris,

FEI) and energy-dispersive X-ray spectrometer (EDS) were also utilized for elemental mapping.

Photocatalytic overall water-splitting tests were conducted in a gas-closed circulation system. The composite photocatalysts (60 mg) were suspended in 12 mL pure water (pH unadjusted) under an argon atmosphere (50 kPa) after repeated evacuation down to 2.5 Pa with constant stirring using a magnetic stirrer. LED lamps with a wavelength of 700 nm (LEDH60-700, Hamamatsu Photonics) was used for light irradiation. The amounts of evolved H_2 and O_2 were monitored using an online gas chromatograph (GC-8A, Shimadzu). We previously reported that the induction period for H_2 and O_2 evolution is up to ~100 h under 700-nm light irradiation;[6,7] however, this delay in H_2 and O_2 evolution disappeared when the water-splitting reaction was allowed to proceed following evacuation of the chamber after ~100 h light irradiation. Thus, in the present study, all of the plotted data for H_2 and O_2 evolution was collected following evacuation of the chamber after ~100 h 700-nm light irradiation.

The apparent quantum efficiency (AQE) values were calculated using the amount of evolved H_2 and the equation: AQE (%) = 100 × 4 × H_2 generation rate/incident photon rate, because H_2 generation in the two-step system is a four-electron process (after reference, Y. Sasaki, H. Nemoto, K. Saito and A. Kudo, *J. Phys. Chem. C*, 2009, **113**, 17536–17542.).

ESI-2) XRD and SEM characterization (Fig. S1).

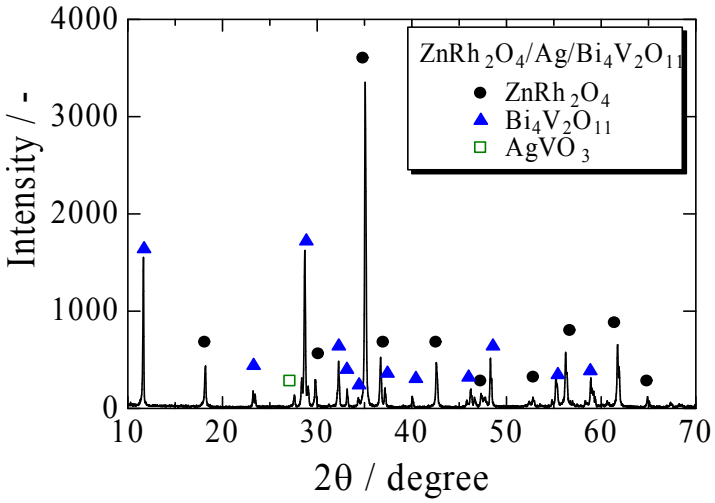

Fig. S1 Powder XRD pattern of $ZnRh_2O_4/Ag/Bi_4V_2O_{11}$.

ESI-3) Bi 4f, Ag 3d, and Pt 4f peak deconvolutions (Fig. S2)

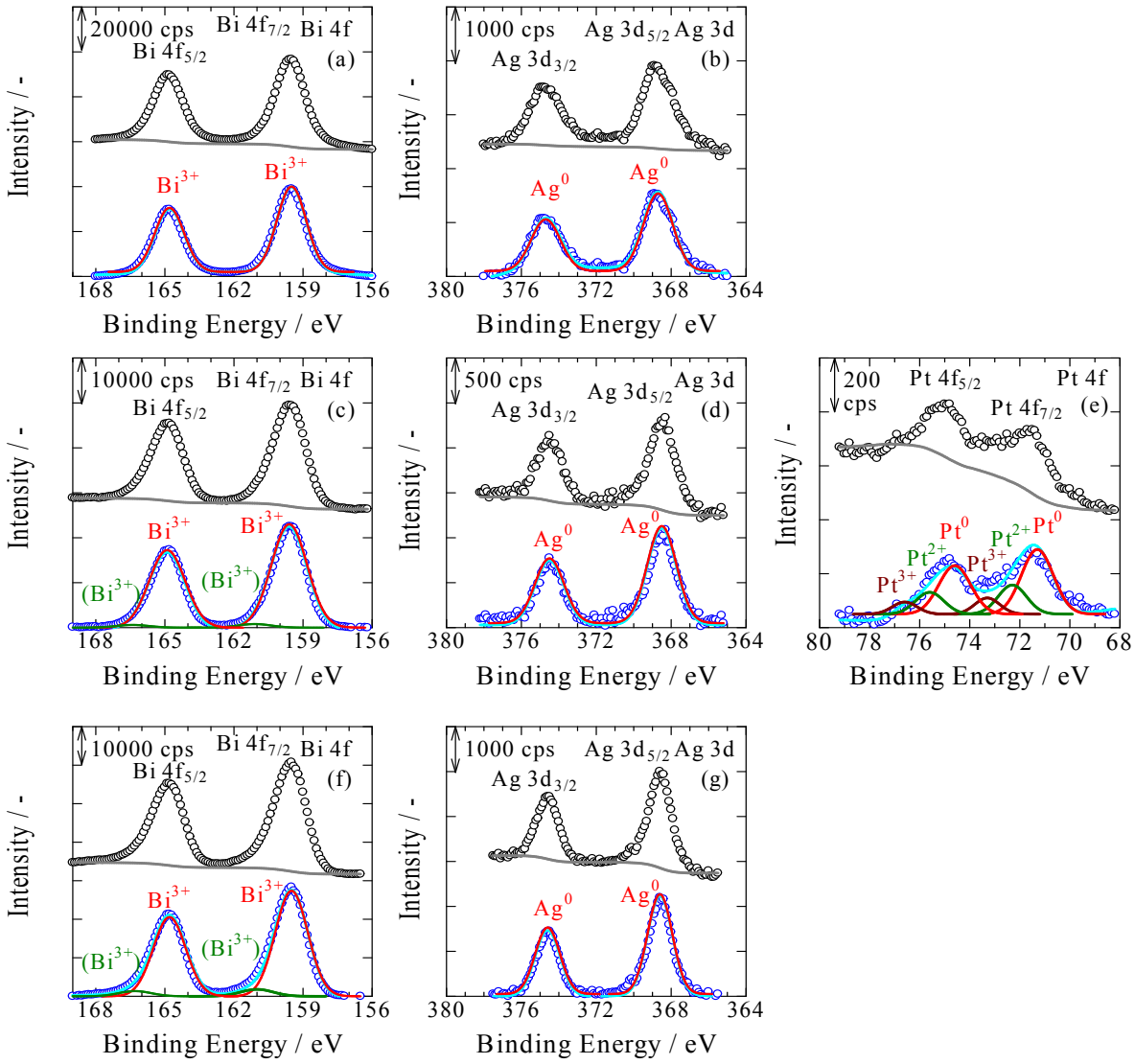

Fig. S2 XPS spectra for Bi 4f (Bi $4_{5/2}$, Bi $4f_{7/2}$) (a) and Ag 3d (Ag $3d_{3/2}$, Ag $3d_{5/2}$) (b) of $ZnRh_2O_4/Ag/Bi_4V_2O_{11}$, Bi 4f (Bi $4f_{5/2}$, Bi $4f_{7/2}$) (c), Ag 3d (Ag $3d_{3/2}$, Ag $3d_{5/2}$) (d) and Pt 4f (Pt $4f_{5/2}$, Pt $4f_{7/2}$) (e) of $Pt/ZnRh_2O_4/Ag/Bi_4V_2O_{11}$, and Bi 4f (Bi $4_{5/2}$, Bi $4f_{7/2}$) (f) and Ag 3d (Ag $3d_{3/2}$, Ag $3d_{5/2}$) (g) of $Ag/ZnRh_2O_4/Ag/Bi_4V_2O_{11}$. The blue open circles in the lower part of each plot were generated by subtracting the background (gray line, upper) from the experimental XPS data (black open plots, upper). The blue open plots and fitted curves (light blue lines, i.e., the sum of the contributions obtained by deconvolution (red, green, and brown lines) closely coincided.

Table S1 Peak deconvolution results for $ZnRh_2O_4/Ag/Bi_4V_2O_{11}$, $Pt/ZnRh_2O_4/Ag/Bi_4V_2O_{11}$, and $Ag/ZnRh_2O_4/Ag/Bi_4V_2O_{11}$. The peak positions (eV), full widths at half maximum (FWHM, eV), and areas for each contribution to the deconvolution, and the peak area ratios of Bi $4f_{5/2}$ to Bi $4f_{7/2}$, Ag $3d_{3/2}$ to Ag $3d_{5/2}$, and Pt $4f_{5/2}$ to Pt $4f_{7/2}$ are also shown.

Photocatalyst		Bi				Ag	
		Bi^{3+}		$Bi^{3+*)}$		Ag^0	
		Bi $4f_{7/2}$	Bi $4f_{5/2}$	Bi $4f_{7/2}$	Bi $4f_{5/2}$	Ag $3d_{5/2}$	Ag $3d_{1/2}$
$ZnRh_2O_4/Ag/Bi_4V_2O_{11}$	BE (eV)	159.5	164.8			368.7	374.7
	FWHM	1.50	1.50			1.83	1.83
	Area	60600	45500			2808	1872
		$(Bi\ 4f_{5/2})/(Bi\ 4f_{7/2})=$	0.75			$(Ag\ 3d_{3/2})/Ag\ 3d_{5/2})=$	0.67
$Pt/ZnRh_2O_4/Ag/Bi_4V_2O_{11}$	BE (eV)	159.6	164.9	161.1	166.4	368.5	374.5
	FWHM	1.83	1.83	1.67	1.67	1.83	1.83
	Area	44800	33600	1420	1060	2110	1410
		$(Bi\ 4f_{5/2})/(Bi\ 4f_{7/2})=$	0.75	$(Bi\ 4f_{5/2})/(Bi\ 4f_{7/2})=$	0.75	$(Ag\ 3d_{3/2})/Ag\ 3d_{5/2})=$	0.67
$Ag/ZnRh_2O_4/Ag/Bi_4V_2O_{11}$	BE (eV)	159.5	164.8	161.0	166.3	368.6	374.6
	FWHM	1.67	1.67	1.66511	1.66511	1.55	1.55
	Area	48600	36400	3190	2390	3660	2440
		$(Bi\ 4f_{5/2})/(Bi\ 4f_{7/2})=$	0.75	$(Bi\ 4f_{5/2})/(Bi\ 4f_{7/2})=$	0.75	$(Ag\ 3d_{3/2})/Ag\ 3d_{5/2})=$	0.67

		Pt					
		Pt^0		Pt^{2+}		Pt^{3+}	
		Pt $4f_{7/2}$	Pt $4f_{5/2}$	Pt $4f_{7/2}$	Pt $4f_{5/2}$	Pt $4f_{7/2}$	Pt $4f_{5/2}$
$ZnRh_2O_4/Ag/Bi_4V_2O_{11}$	BE (eV)						
	FWHM						
	Area						
$Pt/ZnRh_2O_4/Ag/Bi_4V_2O_{11}$	BE (eV)	71.3	74.6	72.3	75.6	73.3	76.6
	FWHM	1.50	1.50	1.33	1.33	1.17	1.17
	Area	383	287	153	115	74	56
		$(Pt\ 4f_{5/2})/(Pt\ 4f_{7/2})=$	0.75	$(Pt\ 4f_{5/2})/(Pt\ 4f_{7/2})=$	0.75	$(Pt\ 4f_{5/2})/(Pt\ 4f_{7/2})=$	0.75
$Ag/ZnRh_2O_4/Ag/Bi_4V_2O_{11}$	BE (eV)						
	FWHM						
	Area						

Table S2 Ag and Pt weight percentages including in $ZnRh_2O_4/Ag/Bi_4V_2O_{11}$, $Pt/ZnRh_2O_4/Ag/Bi_4V_2O_{11}$, and $Ag/ZnRh_2O_4/Ag/Bi_4V_2O_{11}$.

Photocatalyst	Ag / wt%[*1)]	Pt / wt%[*1)]	Inserted Ag / wt%	Ag as a cocatalyst / wt%	Pt as a cocatalyst/ wt%
$ZnRh_2O_4/Ag/Bi_4V_2O_{11}$	2.1		2.1		
$Pt/ZnRh_2O_4/Ag/Bi_4V_2O_{11}$	2.1	1.2	2.1		1.2
$Ag/ZnRh_2O_4/Ag/Bi_4V_2O_{11}$	3.2		2.1[*2)]	1.1[*3)]	

[*1)] Obtained value (vs. 1.0 mol of $ZnRh_2O_4$ + 1.2mol of $Bi_4V_2O_{11}$) from the peak deconvolution results in Table S1.

[*2)] Estimated value based on the assumption that the amount of inserted Ag was identical to that in $ZnRh_2O_4/Ag/Bi_4V_2O_{11}$ and $Pt/ZnRh_2O_4/Ag/Bi_4V_2O_{11}$.

[*3)] Calculated value based on the assumption that the amount of inserted Ag was 2.1 wt%.

ESI-4) SEM images SEM image of the prepared photocatalysts, $ZnRh_2O_4/Ag/Bi_4V_2O_{11}$, $Pt/ZnRh_2O_4/Ag/Bi_4V_2O_{11}$, and $Ag/ZnRh_2O_4/Ag/Bi_4V_2O_{11}$.

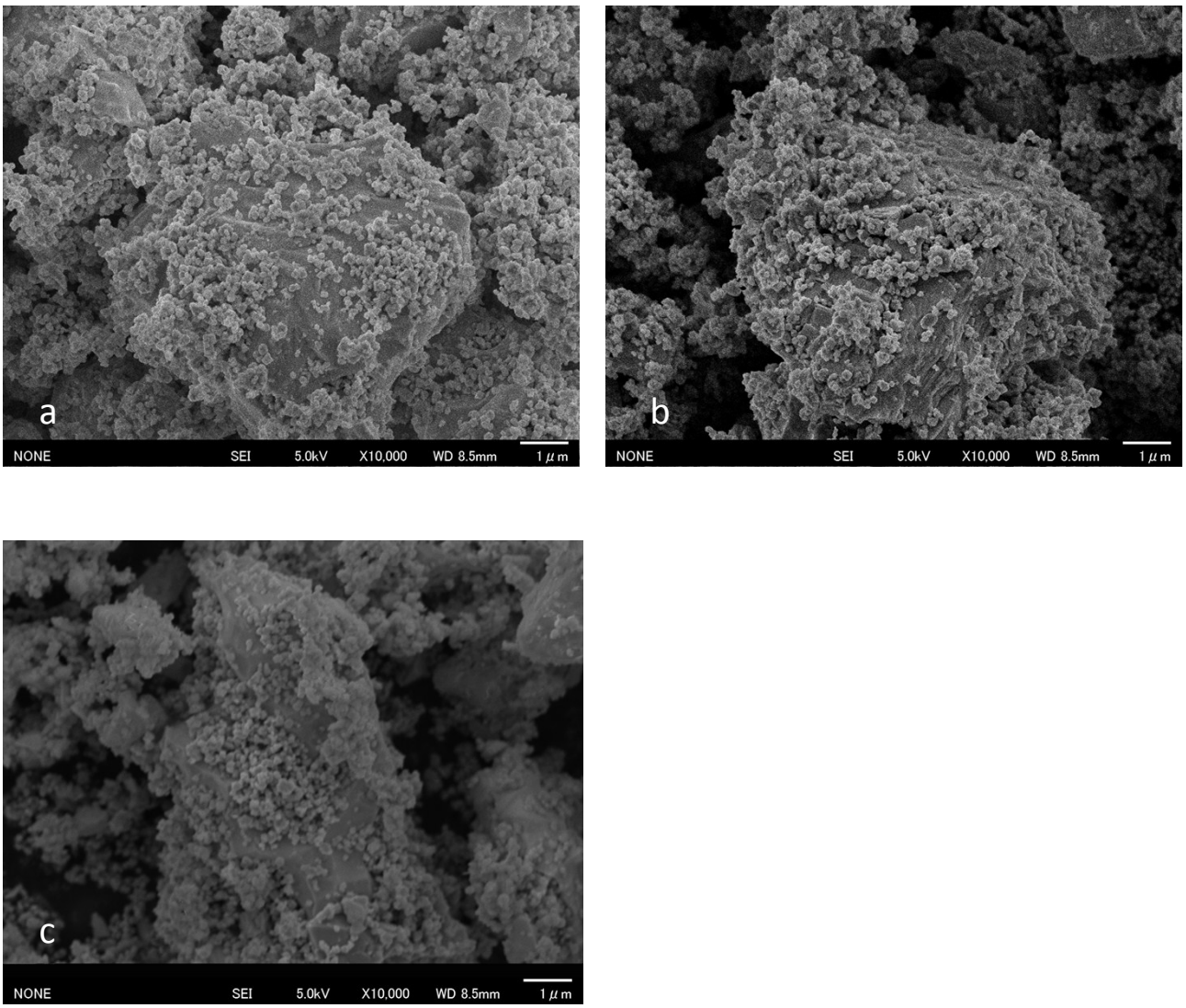

Fig. S3 SEM images of $ZnRh_2O_4/Ag/Bi_4V_2O_{11}$ (a), $Pt/ZnRh_2O_4/Ag/Bi_4V_2O_{11}$ (b), and $Ag/ZnRh_2O_4/Ag/Bi_4V_2O_{11}$ (c).

ESI-5) Enlargement of Figs. 3a-3f (STEM images)

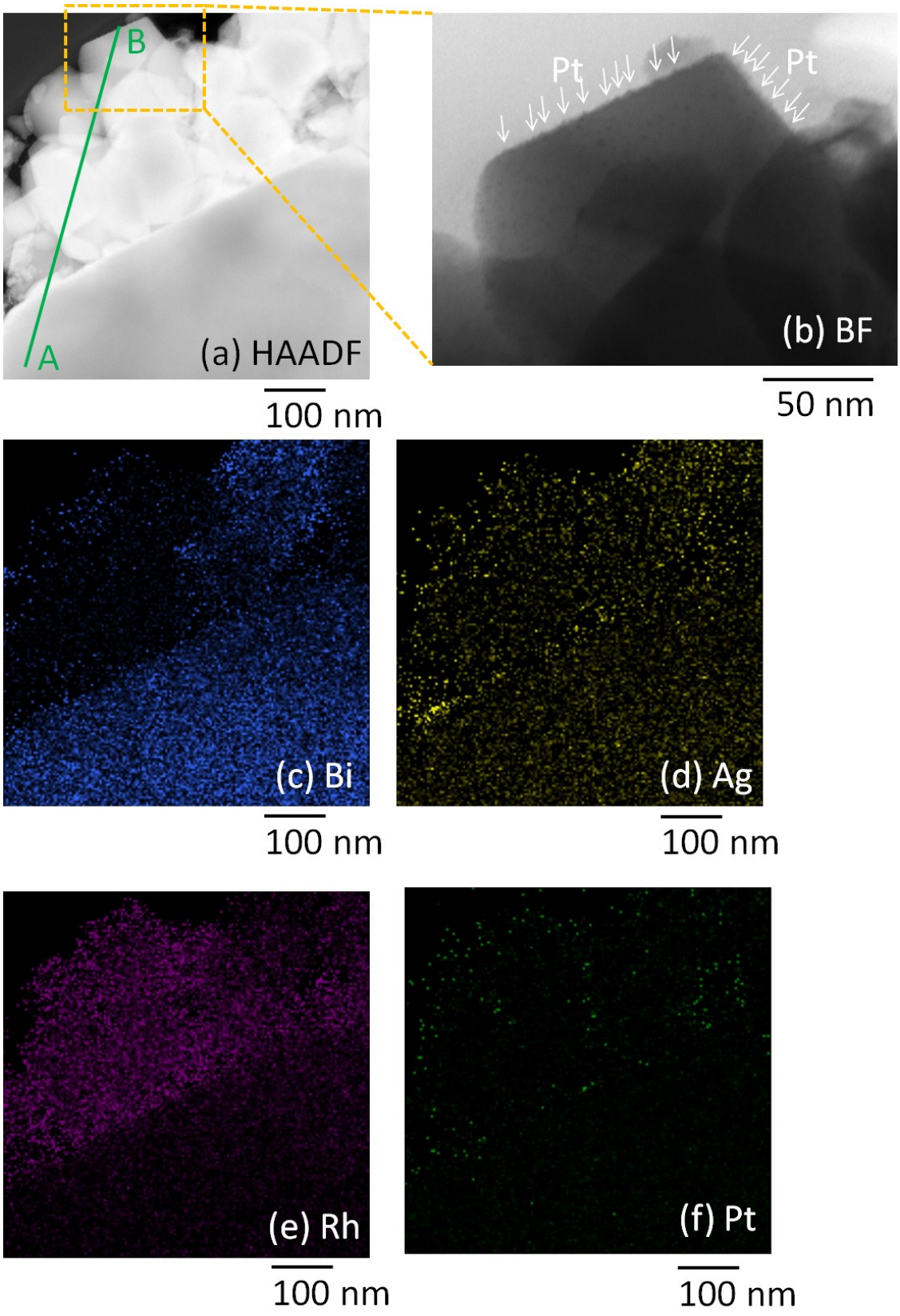

ESI-6) Energy band diagram and charge transfer process for $ZnRh_2O_4$/Ag/$Bi_4V_2O_{11}$ (Scheme S1).

The band edge positions of $ZnRh_2O_4$, Ag, and $Bi_4V_2O_{11}$ are described in Scheme S1a after our previous paper.[9] The band alignments of $ZnRh_2O_4$, Ag, and $Bi_4V_2O_{11}$ before and after the mixing and calcination of Ag and $ZnRh_2O_4$, and Ag and $Bi_4V_2O_{11}$ are shown in Scheme S1b. It should be noted that the uncertainty in the band edge positions for $ZnRh_2O_4$, Ag, and $Bi_4V_2O_{11}$ would correspond to a few tenths of an eV.

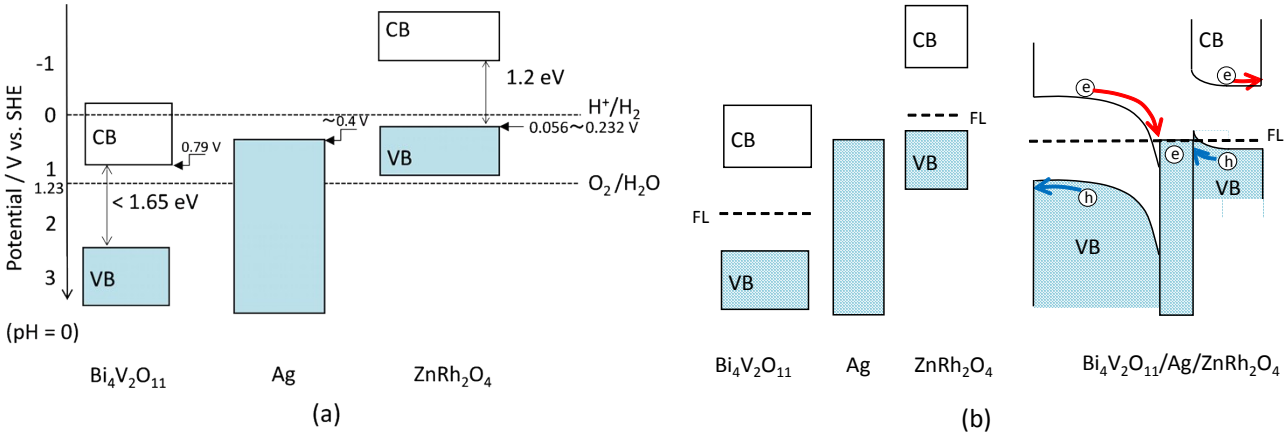

Scheme S1 Band edge positions of $ZnRh_2O_4$, Ag and $Bi_4V_2O_{11}$ (a) and their band alignments before and after the mixing and calcination of Ag and $ZnRh_2O_4$, and Ag and $Bi_4V_2O_{11}$ (b). The charge transfer processes are also shown.

ESI-7) H_2 and O_2 generation rates under 700-nm LED light sources, incident photon rates, and AQE values for overall pure-water splitting (Table S3).

Table S3 Incident photon and H_2 generation rates, and AQE values obtained from H_2 generation rates for overall pure-water splitting over $ZnRh_2O_4/Ag/Bi_4V_2O_{11}$, $Pt/ZnRh_2O_4/Ag/Bi_4V_2O_{11}$, and $Ag/ZnRh_2O_4/Ag/Bi_4V_2O_{11}$.

Photocatalyst	Light intensity / mW cm^{-2}	Incident photon rate / s^{-1}	H_2 generation rate / μmol h^{-1}	AQE (%)
$ZnRh_2O_4/Ag/Bi_4V_2O_{11}$	2.9	7.3×10^{16}	1.7×10^{-2}	1.5×10^{-2}
$Pt/ZnRh_2O_4/Ag/Bi_4V_2O_{11}$	3.5	8.0×10^{16}	5.0×10^{-2}	4.1×10^{-2}
$Ag/ZnRh_2O_4/Ag/Bi_4V_2O_{11}$	3.5	8.0×10^{16}	5.5×10^{-2}	4.6×10^{-2}